AIAA 96-0565
Prediction of Complex Aerodynamic Flows with Explicit Algebraic Stress Models

Ridha Abid
High Technology Corporation
Hampton, VA 23666

Joseph H. Morrison
Analytical Services and Materials, Inc.
Hampton, VA 23666

Thomas B. Gatski
NASA Langley Research Center
Hampton, VA 23681-0001

Charles G. Speziale
Boston University
Boston, MA 02215

34th Aerospace Sciences Meeting & Exhibit
January 15-18, 1996 / Reno, NV

Prediction of Complex Aerodynamic Flows with Explicit Algebraic Stress Models

Ridha Abid*
High Technology Corporation
Hampton, VA 23666

Joseph H. Morrison*
Analytical Sciences and Materials, Inc.
Hampton, VA 23666

Thomas B. Gatski*
NASA Langley Research Center
Hampton, VA 23681-0001

Charles G. Speziale**
Boston University
Boston, MA 02215

Abstract

An explicit algebraic stress equation, developed by Gatski and Speziale, is used in the framework of the $K-\varepsilon$ formulation to predict complex aerodynamic turbulent flows. The nonequilibrium effects are modeled through coefficients that depend nonlinearly on both rotational and irrotational strains. The proposed model was implemented in the ISAAC Navier-Stokes code. Comparisons with the experimental data are presented which clearly demonstrate that explicit algebraic stress models can predict the correct response to nonequilibrium flows.

I. Introduction

Computational fluid dynamics has become an increasingly powerful tool in the aerodynamic design of aerospace vehicles as a result of improvements in numerical algorithms and computer capabilities (e.g., speed, storage). Major future gains in efficiency are expected to come about as massively parallel supercomputer technology matures. However, some critical pacing items limit the effectiveness of computational fluid dynamics in engineering. Chief among these items is turbulence modeling. Numerous turbulence models of varying degrees of complexity, which can be classified as either eddy viscosity or full Reynolds stress models, have been proposed. Excellent reviews of turbulence models have been recently provided by both Speziale[1] and Wilcox.[2]

Eddy viscosity models use the Boussinesq isotropic effective viscosity concept, which assumes that the turbulent stresses in the mean momentum equation are equal to the product of an eddy viscosity and a mean strain rate. Zero-, one-, and two-equation models are among the most popular eddy viscosity models for engineering applications because of their ease of implementation in computational fluid dynamics codes. Algebraic or zero-equation models, which assume local equilibrium of the turbulent and mean flow, have provided reasonable predictions for simple flows. When the turbulent transport is important or the mean conditions change abruptly, these models do not work well. One-equation models improve the predictions for simple near-equilibrium flows but do not account for more complex effects on turbulence. Two-equation models are developed to take explicit account of the history of the turbulence through two transport equations for combinations of the turbulent length and time scales. These models offer good predictions of

* Senior Scientist.
** Professor.

the characteristics and physics of simple separated flows and flows with gradual changes in boundary conditions. However, basic two-equation models fail in many practical flows because they cannot properly account for streamline curvature, rotational strains and buoyancy; they provide an incorrect response to strong adverse pressure gradients; and they cannot describe the anisotropy of turbulence. As a result, various ad hoc modifications to these models have been proposed to achieve the proper response (see Lakshminarayana[3]). In these modifications, effects on turbulence, such as those due to streamline curvature, have been directly accounted for in the eddy viscosity expression or have been reflected indirectly in the turbulence-model equations by modifying the dissipation-rate equation. The improved two-equation models predict a wider range of flows; however, they still fail to properly capture the physics in a broad class of flows. To overcome some of these deficiencies, two-equation turbulence models that are nonlinear in the mean strain rate were proposed by Speziale[4] and Rubinstein and Barton.[5] These models have provided accurate predictions of turbulence intensities. However, these models are not consistent with full Reynolds stress models because they have constant coefficients.

Full Reynolds stress models represent the highest level of closure that is currently feasible for practical calculations. These models are superior to the two-equation models in that they eliminate the assumption that the turbulent stresses respond immediately to changes in the mean strain rate. Also, they account for the anisotropy of turbulence and body force effects on turbulence (e.g., due to streamline curvature and rotation) through extra production terms that explicitly appear in the Reynolds stress transport equation. However, models for many unknown turbulent quantities are required. This need is generally met by assuming that the turbulence is locally homogeneous and in equilibrium. Existing Reynolds stress models have been shown to give good descriptions of two-dimensional mean turbulent flows that are near equilibrium. However, computer costs and numerical stability problems that arise from the absence of a turbulent viscosity make assessments of the limitations of these models in predicting complex flows difficult. However, second-order closure models could be used to derive better two-equation models because fundamentally they are constructed on a stronger theoretical basis than the lower level models.

Recently, a methodology for deriving a general nonlinear constitutive relation (or an explicit algebraic stress equation) for the Reynolds stress tensor from second-order closures, has been proposed by Gatski and Speziale,[6] based on the ideas of Pope.[7] This derivation is based on the assumptions that the net convection of the turbulent stresses is proportional to the net convection of the turbulent kinetic energy and that the structural parameters of the turbulence are constant along a streamline. As a result, a new generation of non-linear two-equation models is obtained with coefficients that depend on rotational and irrotational strains. This new feature extends the range of applicability of the standard two-equation models.

Abid et al.[8] used the explicit algebraic stress relation within the context of the K–ω and K–ε two-equation format to predict separated airfoil flows. The Launder, Reece and Rodi[9] pressure-strain correlation model was considered in the above study. Comparisons with the experimental data have shown that this new nonlinear turbulence model improves the ability of two-equation models to account for nonequilibrium effects. However, the Reynolds stress anisotropies were not well predicted.

In this paper, the algebraic stress relation is applied within the context of the K–ε two-equation format using the Speziale, Sarkar and Gatski[10] pressure-strain correlation model. The ability of the proposed model to predict complex flows which include nonequilibrium and anisotropic effects is assessed. Transonic flows over two airfoils and a wing are considered in this study. The ISAAC Navier-Stokes code is used to compute the three test cases.

II. Theoretical Analysis

For a weakly compressible turbulent flow at high Reynolds numbers, the Reynolds stress tensor $\tau_{ij} = \overline{u_i u_j}$ is a solution of the transport equation[11]

$$\frac{D\tau_{ij}}{Dt} = -\tau_{ik}\frac{\partial \overline{u}_j}{\partial x_k} - \tau_{jk}\frac{\partial \overline{u}_i}{\partial x_k} + \frac{\Pi_{ij}}{\overline{\rho}} - \frac{2}{3}\varepsilon\delta_{ij} + D_{ij}^T + \nu\nabla^2\tau_{ij} \quad (1)$$

given that Π_{ij} is the pressure-strain correlation, D_{ij}^T is the turbulent transport term, ε is the turbulent dissipation-rate, ν is the kinematic viscosity, $\overline{u}_i$ is the mean-velocity component, and $\overline{\rho}$ is the mean density. Explicit compressibility effects are neglected in Eq. (1) due to the applicability of Markovin's hypothesis in these weakly compressible flows.

If we contract the indices in (1), then we obtain the transport equation for the turbulent kinetic energy $K = \overline{u_i u_i}/2$:

$$\frac{DK}{Dt} = P - \varepsilon + D_K^T + \nu\nabla^2 K \quad (2)$$

given that $P = -\tau_{ij}\left(\partial \overline{u}_i/\partial x_j\right)$ is the turbulence production term and D_K^T is the turbulent transport term.

Rodi[12] proposed the idea of algebraic stress closure, which provides algebraic equations without solving differential equations for the Reynolds stresses. He assumed that

$$\frac{D\tau_{ij}}{Dt} - \nu\nabla^2\tau_{ij} - D_{ij}^T = \frac{\tau_{ij}}{K}\left(\frac{DK}{Dt} - D_K^T - \nu\nabla^2 K\right) \quad (3)$$

and

$$\frac{Db_{ij}}{Dt} = 0 \quad (4)$$

where

$$b_{ij} = \frac{\tau_{ij} - \frac{2}{3}K\delta_{ij}}{2K} \quad (5)$$

is the Reynolds stress anisotropy. Physically, two assumptions are made in the algebraic Reynolds stress closures: the convection term minus the diffusion term in the Reynolds stress equation is proportional to the convection term minus the diffusion term in the turbulent kinetic energy equation and the Reynolds stress anisotropy b_{ij} is constant along a streamline.

The substitution of (3) and (4) into (1) yields the following algebraic stress equation:

$$(P-\varepsilon)b_{ij} = -\frac{2}{3}KS_{ij} - K\left(b_{ik}S_{jk} + b_{jk}S_{ik} - \frac{2}{3}b_{mn}S_{mn}\delta_{ij}\right) - K\left(b_{ik}W_{jk} + b_{jk}W_{ik}\right) + \frac{\Pi_{ij}}{2\overline{\rho}} \quad (6)$$

where

$$S_{ij} = \frac{1}{2}\left(\frac{\partial \overline{u}_i}{\partial x_j} + \frac{\partial \overline{u}_j}{\partial x_i}\right) \quad (7)$$

and

$$W_{ij} = \frac{1}{2}\left(\frac{\partial \overline{u}_i}{\partial x_j} - \frac{\partial \overline{u}_j}{\partial x_i}\right) \quad (8)$$

are the mean-rate-of-strain tensor and mean-vorticity tensor, respectively.

Given a pressure-strain-correlation model, (6) provides an implicit algebraic equation for the determination of the Reynolds stress τ_{ij}. Computations that use this model have shown that stable numerical solutions can be difficult to obtain. Hence, an explicit algebraic stress equation which is a mathematically consistent representation of (6) is preferable.

Pope[7] developed a methodology for obtaining explicit algebraic stress equations by using a tensorial polynomial expansion in the integrity basis.[5] Gatski and Speziale[6] used this method to derive an explicit algebraic stress equation for two- and three-dimensional turbulent flows. In order to generalize their results, they applied their algebraic stress representation to the general class of pressure-strain correlation models for Π_{ij} which are linear in the anisotropic tensor b_{ij}. The general linear form of Π_{ij} is

$$\frac{\Pi_{ij}}{\bar{\rho}} = -C_1\varepsilon b_{ij} + C_2 K S_{ij} + C_3 K\Big(b_{ik}S_{jk} + b_{jk}S_{ik} - \frac{2}{3}b_{mn}S_{mn}\delta_{ij}\Big) + C_4 K\big(b_{ik}W_{jk} + b_{jk}W_{ik}\big) \quad (9)$$

The explicit nonlinear constitutive equation, derived by Gatski and Speziale,[6] is then given after regularization by

$$\bar{\rho}\tau_{ij} = \frac{2}{3}\bar{\rho}K\delta_{ij} - 2\mu_t\Big[\Big(S_{ij} - \frac{1}{3}S_{kk}\delta_{ij}\Big) + \frac{\alpha_4}{\omega}\big(S_{ik}W_{kj} + S_{jk}W_{ki}\big) - \frac{\alpha_5}{\omega}\Big(S_{ik}S_{kj} - \frac{1}{3}S_{k\ell}S_{k\ell}\delta_{ij}\Big)\Big] \quad (10)$$

with

$$\mu_t = \bar{\rho}C_\mu^* \frac{K}{\omega} \quad (11)$$

$$C_\mu^* = \frac{3\big(1+\eta^2\big)\alpha_1}{3+\eta^2+6\eta^2\xi^2+6\xi^2} \quad (12)$$

$$\eta^2 = \frac{\alpha_2}{\omega^2}\big(S_{ij}S_{ij}\big), \quad \xi^2 = \frac{\alpha_3}{\omega^2}\big(W_{ij}W_{ij}\big) \quad (13)$$

where $\bar{\rho}$ is the mean density and $\omega = \varepsilon/K$ is the specific dissipation rate. The constants in (11)–(13) are given by

$$\alpha_1 = \Big(\frac{4}{3} - C_2\Big)\frac{g}{2}, \quad \alpha_2 = \big(2-C_3\big)^2\frac{g^2}{4} \quad (14)$$

$$\alpha_3 = \big(2-C_4\big)^2\frac{g^2}{4}, \quad \alpha_4 = \Big(\frac{2-C_4}{2}\Big)g \quad (15)$$

$$\alpha_5 = \big(2-C_3\big)g, \quad g = \frac{1}{\frac{C_1}{2}+C_5-1} \quad (16)$$

To avoid numerical problems in the initial stages of the computation or in the free-stream region, a modified form of C_μ^* is used

$$C_\mu^* = \alpha_1\frac{3\big(1+\eta^2\big)+0.2\big(\eta^6+\xi^6\big)}{3+\eta^2+6\eta^2\xi^2+6\xi^2+\eta^6+\xi^6} \quad (17)$$

which is equivalent to Eq. (12) to order η^4 and ξ^4. Relation (17) does not change the value of C_μ^* near equilibrium conditions, but limits C_μ^* to a small non-zero value (= $0.2\alpha_1$) for high values of η or ξ to avoid numerical instabilities. In the present study, the pressure-strain-correlation model of Speziale, Sarkar, and Gatski[10] is considered; the coefficients are:

$$C_1 = 6.8, \quad C_2 = 0.36, \quad C_3 = 1.25,$$
$$C_4 = 0.40, \quad C_5 = 1.88 \quad (18)$$

The nonlinear constitutive equation (10) must be solved in conjunction with the following modeled transport equations.

$$\bar{\rho}\frac{DK}{Dt} = \bar{\rho}P - \bar{\rho}\varepsilon + \frac{\partial}{\partial x_j}\Big(\Big(\mu_\ell + \frac{\mu_{t\ell}}{\sigma_k}\Big)\frac{\partial K}{\partial x_j}\Big) \quad (19)$$

and

$$\bar{\rho}\frac{D\varepsilon}{Dt} = C_{\varepsilon_1}\bar{\rho}\frac{\varepsilon}{K}P - C_{\varepsilon_2}\bar{\rho}f\frac{\varepsilon^2}{K} + \frac{\partial}{\partial x_j}\Big(\Big(\mu_\ell + \frac{\mu_{t\ell}}{\sigma_\varepsilon}\Big)\frac{\partial\varepsilon}{\partial x_j}\Big) \quad (20)$$

given that $\mu_{t\ell} = C_{\mu\ell}^*\bar{\rho}\frac{K^2}{\varepsilon}$ and $C_{\mu\ell}^*(=0.081)$ is the value of C_μ^* in the logarithmic layer. The coefficients of the model are

$$\sigma_k = 1.0, \quad \kappa = 0.40, \quad C_{\varepsilon_2} = 1.83, \quad C_{\varepsilon_1} = 1.44$$

$$\sigma_\varepsilon = \frac{\kappa^2}{\big(C_{\varepsilon_2} - C_{\varepsilon_1}\big)\sqrt{C_{\mu\ell}^*}} \quad (21)$$

and

$$f = \Big[1-\exp\Big(-\frac{y^+}{5.5}\Big)\Big]^2, \quad y^+ = \frac{\rho y u_\tau}{\mu} \quad (22)$$

given that u_τ is the shear velocity and y is normal to the wall. Note that new model can be integrated directly to the wall without adding a damping to the eddy viscosity. The function f is introduced to remove the singularity in the dissipation rate equation at the wall.

At the wall, the boundary conditions for K and ε are

$$K = 0, \qquad \varepsilon = 2\nu\left(\frac{\partial\sqrt{K}}{\partial y}\right)^2 \tag{23}$$

III. Results and Discussion

The calculations to be presented were done with the three-dimensional Navier-Stokes ISAAC code,[13] which uses a second-order accurate finite-volume scheme. The convective terms are discretized with an upwind scheme that is based on Roe's flux-difference splitting method. All viscous terms are centrally differenced. The equations are integrated in time with an implicit, spatially split approximate-factorization scheme.

The performance of the explicit algebraic turbulence model (hereafter referred to as EASM) was evaluated for the flat-plate turbulent boundary layer at a zero-pressure gradient. As expected (the results are not shown here), the turbulence model yielded good predictions for the mean-velocity profiles and skin-friction coefficients. Although some turbulence properties near the wall are not captured (i.e., the peak of the turbulent kinetic energy), the algebraic stress model does give accurate results away from the buffer layer (i.e., $y^+ > 30$). Remember that the algebraic stress model can be integrated directly to a solid boundary with no damping function in the turbulent eddy viscosity.

The first two test cases to be considered are the RAE 2822 airfoil flows (cases 9 and 10), which were tested by Cooke et al.[14] The airfoil has a maximum thickness of 12.1 percent c and a leading-edge radius of 0.827 percent c (c is the chord of the airfoil). The grid used is a 257×97 C mesh with 177 points on the airfoil, and a minimum spacing at the wall of $0.932\times10^{-6}c$. The outer boundary extent is approximately $18c$, and transition is assumed at 3 percent c. For the case 9, the conditions include a Mach number $M_\infty = 0.73$, an angle of attack $\alpha = 2.8°$, and a Reynolds number $Re = 6.5\times10^6$. This case contains no separated flow. For the case 10, the conditions include a Mach number $M_\infty = 0.75$, an angle of attack $\alpha = 2.72$, and a Reynolds number $Re = 6.2\times10^6$. This case involves separation based on visual surface streamline patterns. However, there are no skin-friction coefficient data indicating separation. Hence, case 10 is considered as an incipiently separated flow and, therefore, is more challenging than the previous case.

Figures 1 and 2 compare the surface pressure and skin-friction coefficients computed along the airfoil surface with the experimental data for case 9. It is clear that the explicit algebraic stress model provides a good representation of the pressure over most of the airfoil. However, the turbulence model over predicts the skin-friction coefficient downstream of the shock. This deficiency results from the tendency of the models based on K–ε formulation to predict excessive near-wall levels of turbulent length scale in the presence of an adverse pressure gradient, which leads to high values of the eddy-viscosity. A modification of the dissipation equation is required in order to improve the response of the algebraic stress model to adverse pressure-gradient effects.

In order to demonstrate the improvement resulting from the use of the EASM model for non-equilibrium flows, comparisons between the results obtained by the EASM model and the Speziale, Abid and Anderson $K-\varepsilon$ model[15] (hereafter referred to as SAA) were performed (Figures 3–10). From Figure 4, it appears clearly that neither turbulence model predicts separation. This is reflected by the high level of the skin-friction coefficient, downstream from the shock. This probably is a result of the inability of the length scale equation to provide proper response to adverse pressure gradients. To date, several modifications to the dissipation equation for separation do not seem to be successful. On the other hand, the EASM model predicts the shock location better than the SAA model, although slightly downstream of the experimental shock location (see Figure 3). This results from the prediction by the EASM of lower values of eddy viscosity in the inner part of the boundary layer, therefore, lower values of the turbulent kinetic energy (see Figure 7). Comparison of the computed and measured

velocity profiles further support the latter observation. An additional finding that can be inferred from the above comparison is that the EASM model gives a realistic representation of the normal stresses (see Figures 8–10).

The third test case to be considered is the ONERA M6 wing at Mach number of 0.8447, an angle of attack α of 5.06 and a Reynolds number of 11.7×10^6 based on the mean aerodynamic chord.[16] A C–O grid, used in this study has 193×49×33 points in the streamwise, normal and spanwise direction. The minimum normal spacing over the wing of 0.000015 c_{root} and a distance from the wing to the outer boundary of at least 7.95 c_{root} . No wind tunnel test corrections are employed for this case.

Figure 11 shows a comparison of the surface pressure distributions with the experimental data at four different spanwise locations $2y/B$. It is clear from this figure, that the predicted shock location and the surface pressure distributions by the EASM model are in good agreement with the experimental data, and similar to the results reported in [17] for the Johnson-King model, which has been highly tuned for airfoil flows.

Conclusions

A study of an explicit algebraic stress model, used in the framework of the $K-\varepsilon$ formulation for separated turbulent flows, has been conducted. This new generation of two-equation models, which is derived from second-order closures, has been tested against three test cases, two of which involve separation. Two major findings have been made in this study: explicit algebraic stress models have shown some improvement over the standard two-equation models because of their ability to account for nonequilibrium effects and to give a realistic representation of the anisotropy of the turbulence. However, this improvement is still limited by the dissipation rate equation which fails to respond properly to adverse pressure gradients. A major research effort to correct this deficiency is currently underway.

Acknowledgements

The first and second authors (RA and JHM) would like to thank NASA Langley Research Center for support under contracts NAS1-20059 and NAS1-19831. The fourth author (CGS) acknowledges the support of the Office of Naval Research under Grant No. N00014-94-1-0088 (Dr. L. P. Purtell, Program Officer).

References

[1]Speziale, C. G., "Analytical methods for the development of Reynolds stress closures in turbulence," *Ann. Rev. Fluid Mech.* **23**, 107–157, 1991.

[2]Wilcox, D. C., *Turbulence Modeling for CFD*, DCW Industries, Inc., LaCanada, CA, 1993.

[3]Lakshminarayana, B., "Turbulence modelling for complex flows," AIAA-85-1652, 1985.

[4]Speziale, C. G., "On nonlinear $K-\ell$ and $K-\varepsilon$ models of turbulence," *J. Fluid Mech.* **178**, 459, 1987.

[5]Rubinstein, R., and Barton, J. M., "Nonlinear Reynolds stress models and the normalization group," *Phys. Fluids* **A2**, 1472, 1990.

[6]Gatski, T. B., and Speziale, C. G., "On explicit algebraic stress models for complex turbulent flows," *J. Fluid Mech.* **254**, 59–78, 1993.

[7]Pope, S. B., "A more general effective viscosity hypothesis," *J. Fluid Mech.* **72**, 331–340, 1975.

[8]Abid, R., Rumsey, C., and Gatski, T. B., "Prediction of Non-Equilibrium Turbulent Flows with Explicit Algebraic Stress Models," *AIAA J.* **33**(11), Nov. 1995.

[9]Launder, B. E., Reece, G. J., and Rodi, W., "Progress in the development of a Reynolds stress turbulence closure," *J. Fluid Mech.* **68**, 537–566, 1975.

[10]Speziale, C. G., Sarkar, S., and Gatski, T. B., "Modeling the pressure-strain correlation of turbulence: an invariant dynamical system approach," *J. Fluid Mech.* **227**, 245–272, 1991.

[11]Hinze, J. O., *Turbulence*, McGraw-Hill, 1975.

[12]Rodi, W., "A new algebraic relation for calculating the Reynolds stresses," *Z. Angew. Math Mech.* **56**, T219–T221, 1976.

[13]Morrison, J. H., "A compressible Navier-Stokes solver with two-equation and Reynolds stress turbulence closure models," NASA CR4440, May 1992.

[14]Cooke, P., McDonald, M., and Firmin, M., "Airfoil RAE2822—pressure distributions and boundary layer wake measurements," AGARD AR-138, 1979.

[15]Speziale, C. G., Abid, R., and Anderson, E. C., "Critical evaluation of two-equation models for near-wall turbulence," *AIAA J.* **30**(2), 324–331, 1992.

[16]Schmitt, V. and Charpin, F., "Pressure distribution on the ONERA M6 wing at transonic Mach numbers," AGARD-AR-138, May 1979.

[17]Rumsey, C. and Vatsa, V. N., "A comparison of the predictive capabilities of several turbulence models using upwind and central-difference computer codes," AIAA 93–0192.

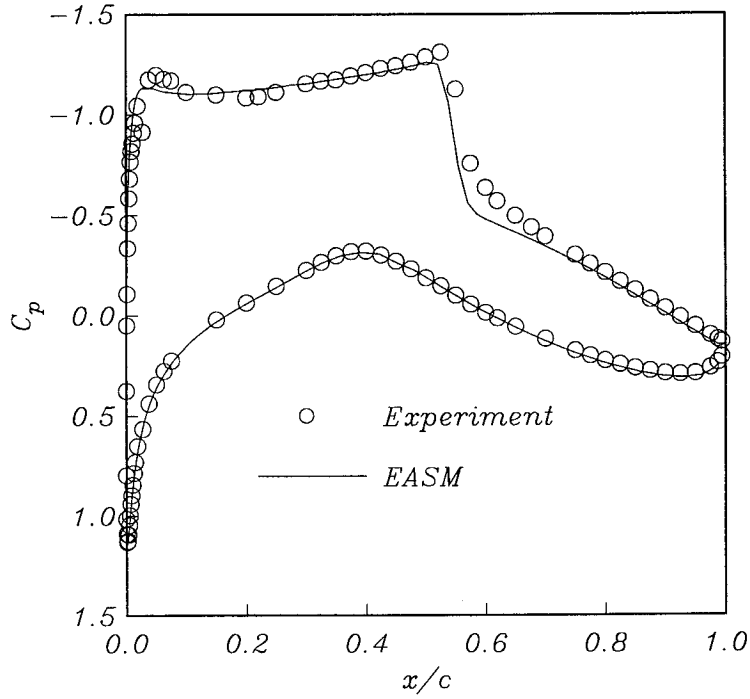

Figure 1: Surface pressure distributions for RAE 2822 airfoil (Case 9)

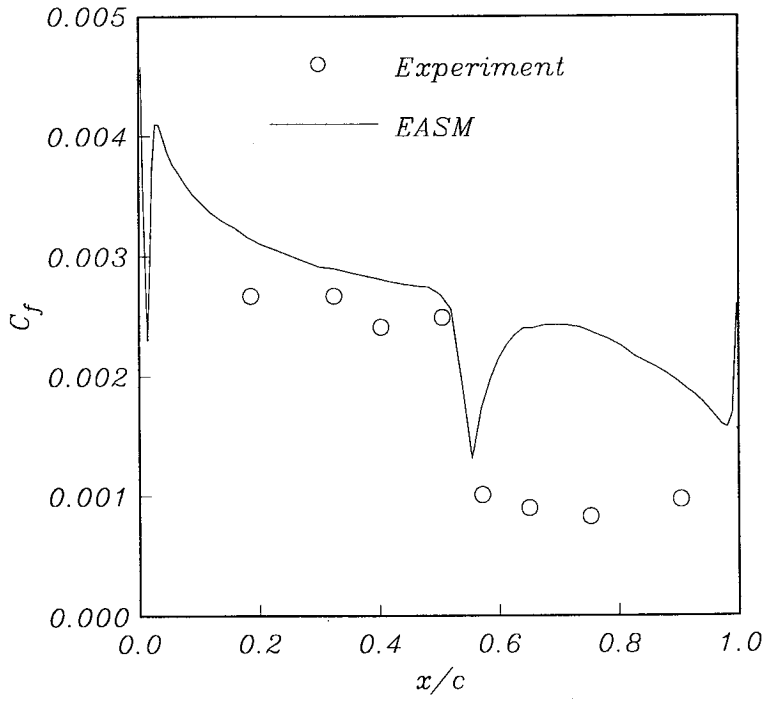

Figure 2: Skin friction distributions for RAE 2822 airfoil (Case 9)

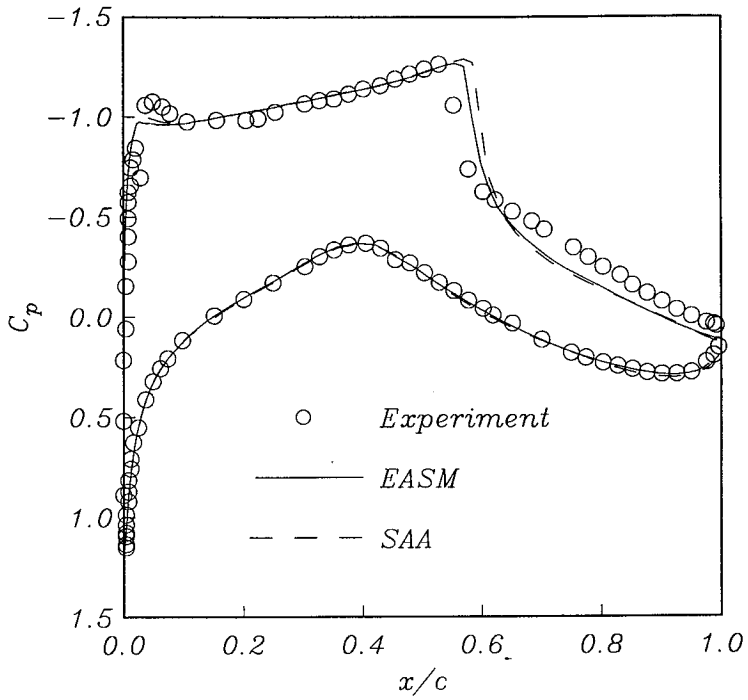

Figure 3: Surface pressure distributions for RAE 2822 airfoil (Case 10)

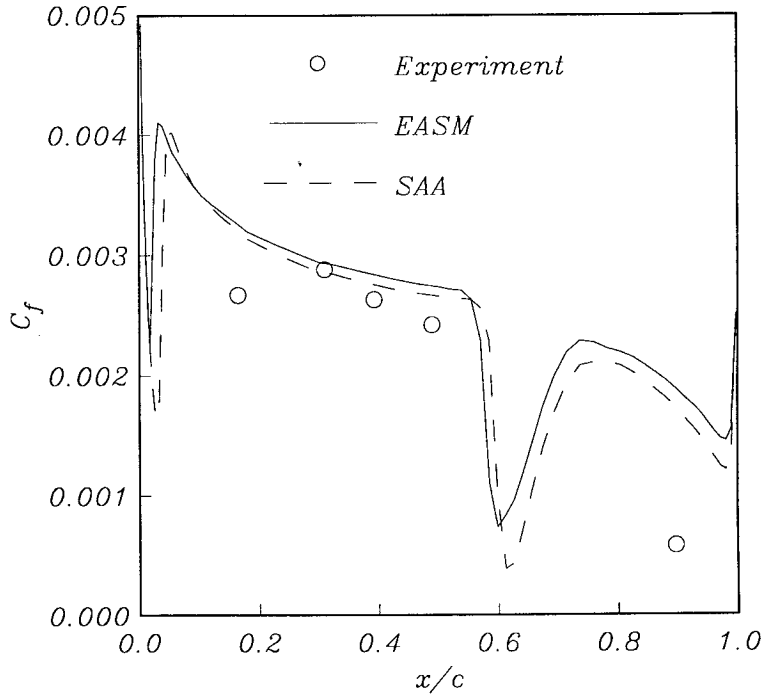

Figure 4: Skin friction distributions for RAE 2822 airfoil (Case 10)

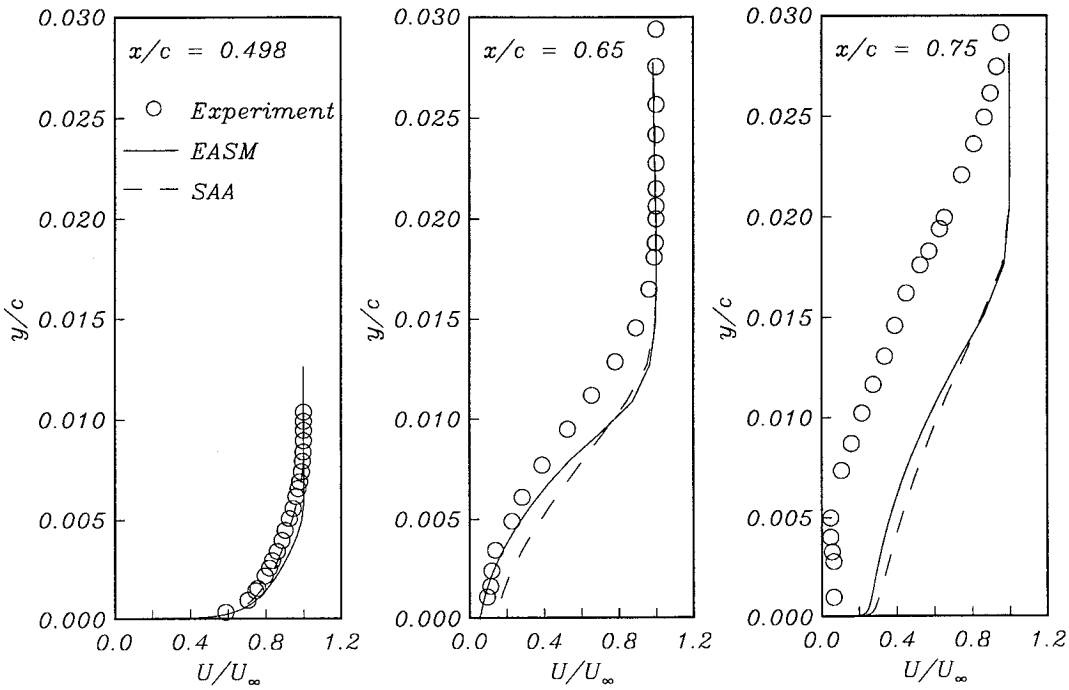

Figure 5: Comparison of mean velocity profiles for RAE 2822 airfoil (Case 10)

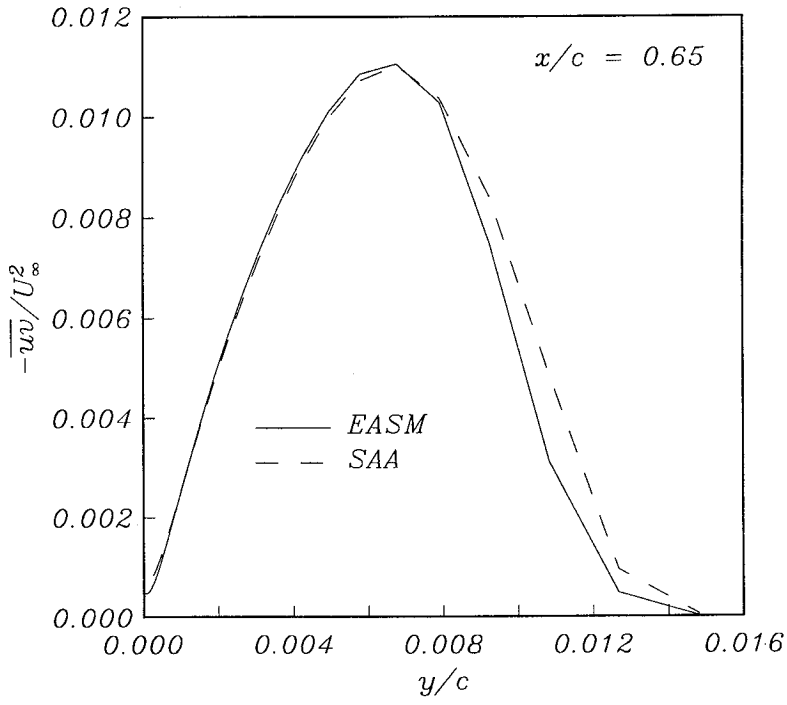

Figure 6: Comparison of turbulent shear stress distributions for RAE 2822 airfoil (Case 10)

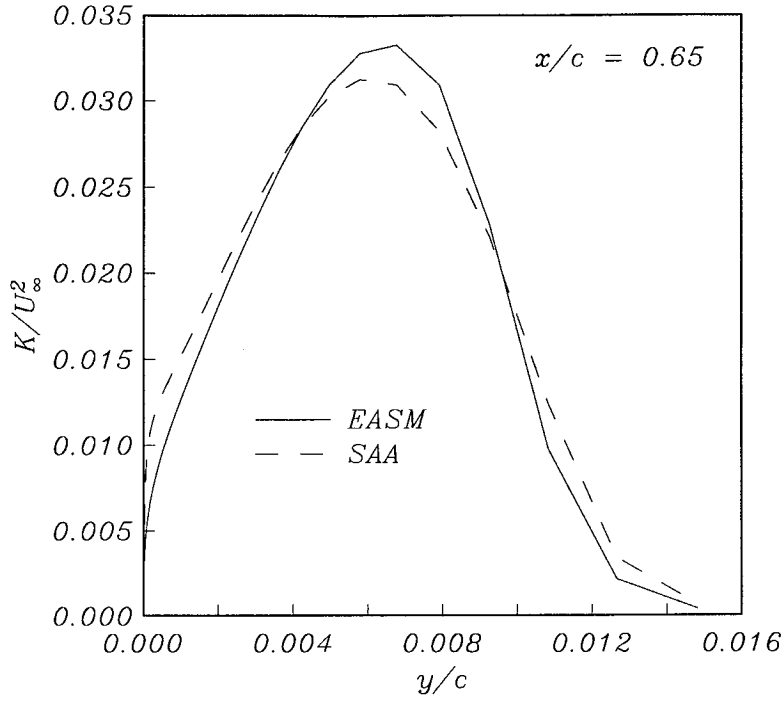

Figure 7: Comparison of turbulent kinetic energy distributions for RAE 2822 airfoil (Case 10)

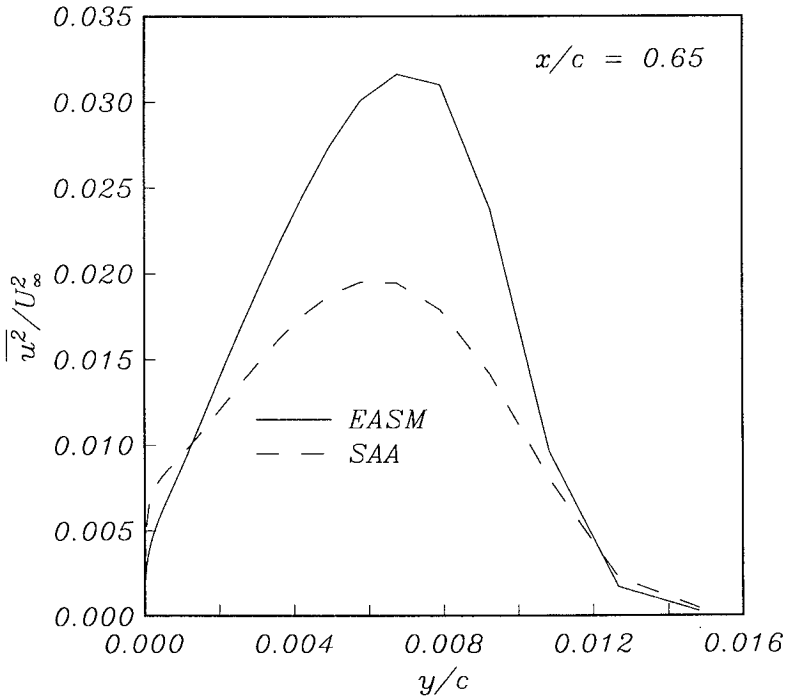

Figure 8: Comparison of $\overline{u^2}$ normal stress distributions for RAE 2822 airfoil (Case 10)

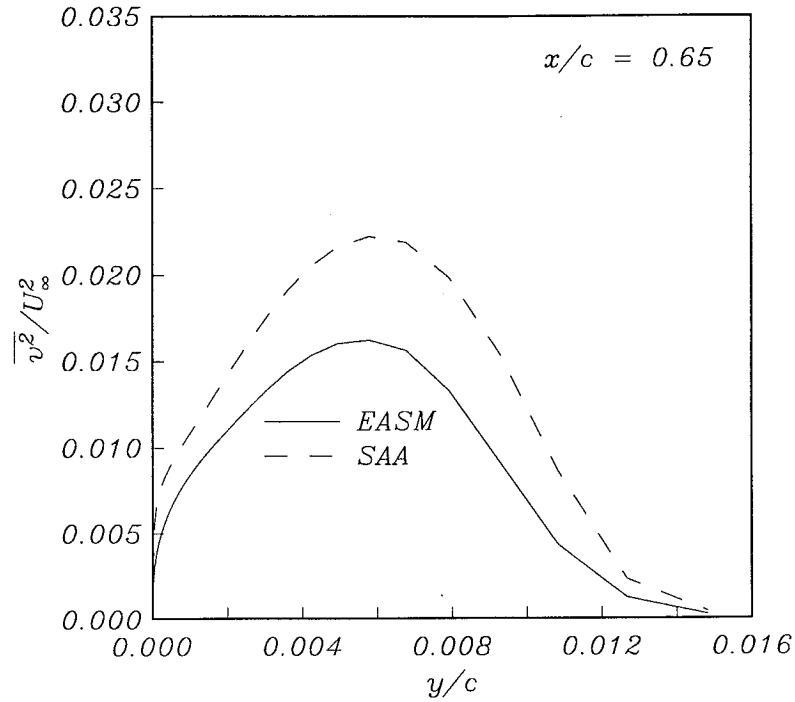

Figure 9: Comparison of $\overline{v^2}$ normal stress distributions for RAE 2822 airfoil (Case 10)

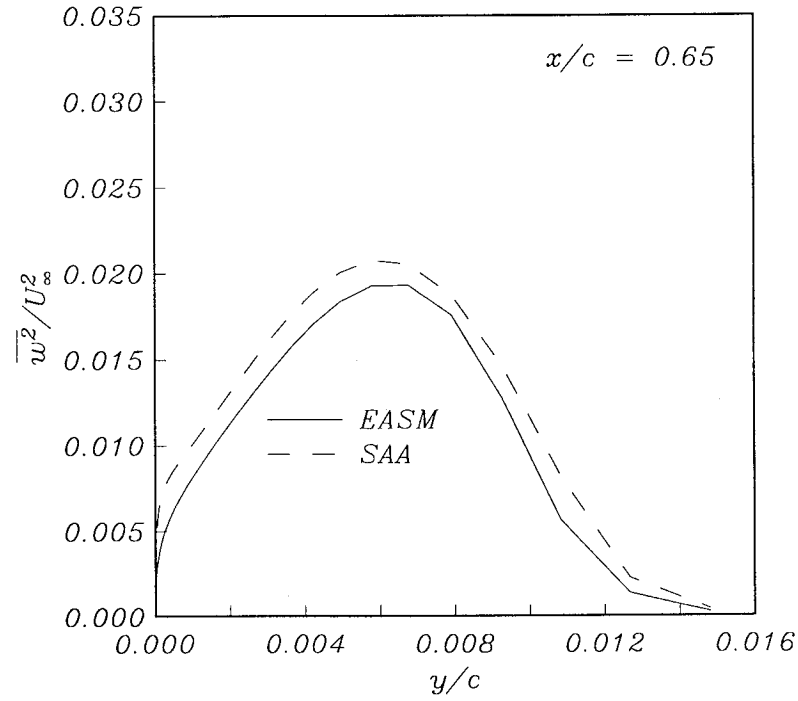

Figure 10: Comparison of $\overline{w^2}$ normal stress distributions for RAE 2822 airfoil (Case 10)

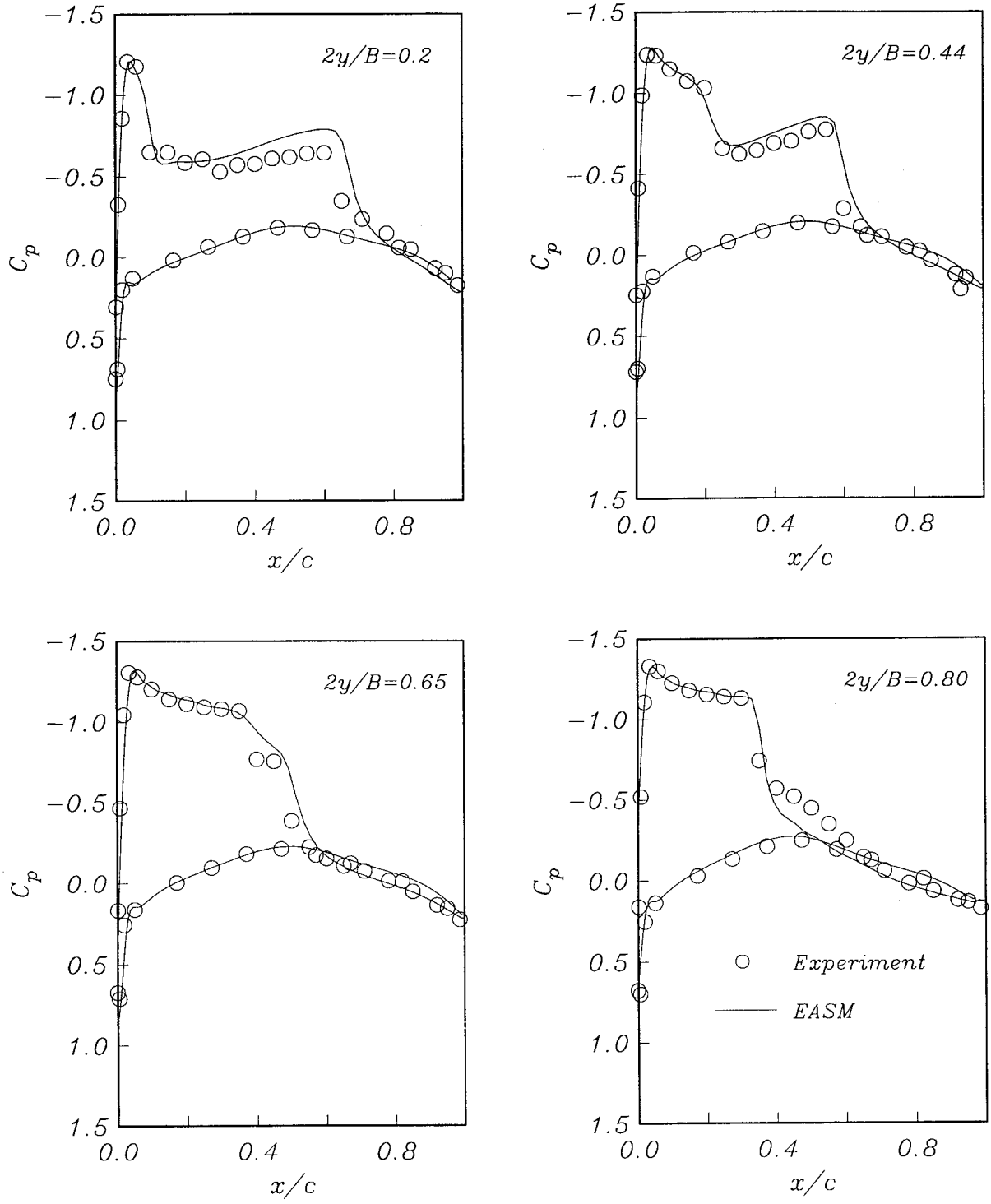

Figure 11: Surface pressure distributions for ONERA M6 wing